

Thermal conductivity and specific heat capacity of water–ethylene glycol mixture-based nanofluids with graphene nanoplatelets

C. Selvam¹ · D. Mohan Lal¹ · Sivasankaran Harish²

Received: 19 September 2016 / Accepted: 6 March 2017 / Published online: 20 March 2017
© Akadémiai Kiadó, Budapest, Hungary 2017

Abstract In the present work, we report the thermal conductivity and specific heat capacity of water–ethylene glycol mixture with graphene nanoplatelets inclusions. Stable nanofluid dispersions were prepared with sodium deoxycholate as the surfactant. Stability of nanofluids was characterized by optical absorption spectroscopy and zeta potential analysis. Thermal conductivity of nanofluids was found to increase with respect to nanoplatelets loading, while the specific heat capacity was decreasing. Highest enhancement in thermal conductivity of nanofluid was found to be $\sim 18\%$ at 0.45 vol% of nanoplatelets loading while at the same concentration the specific heat capacity was $\sim 8\%$ lower. Further measured thermal conductivity was compared with effective medium theory calculations considering the role of interfacial thermal resistance. From the model calculations, we show that the interfacial thermal resistance between graphene nanoplatelets and water–ethylene glycol mixture was significantly high in the order of $1.7 \times 10^{-8} \text{ m}^2 \text{ K W}^{-1}$ which limits the thermal conductivity enhancement despite the high intrinsic thermal conductivity of graphene nanoplatelets.

Keywords Thermal conductivity · Specific heat capacity · Graphene nanoplatelets · Nanofluid

Abbreviations

GnP	Graphene nanoplatelets
GnP/H ₂ O–	Graphene/water–ethylene glycol nanofluid
EG	
EG	Ethylene glycol
H ₂ O	Water
SDC	Sodium deoxycholate
SWCNT	Single-walled carbon nanotubes
vol%	Volume fraction of the nanomaterial
mass%	Weight fraction of the nanomaterial

List of symbols

C_p	Specific heat capacity ($\text{kJ kg}^{-1} \text{K}^{-1}$)
k	Thermal conductivity ($\text{W m}^{-1} \text{K}^{-1}$)

Greek symbols

ρ	Density (g cm^{-3})
φ	Volume fraction (%)

Subscripts

bf	Basefluid
nf	Nanofluid
P	Nanoparticle

Introduction

Energy transport is continuously facing challenges in various industries for cooling and heating applications. Energy transport with conventional heat transfer fluids are widely used in many industries and different thermal systems. However, the thermal conductivity of conventional heat transfer fluids is limited resulting in poor heat transfer performance. The fluids having high thermal conductivity are needed to enhance the energy transfer rate of compact

✉ D. Mohan Lal
mohanlal@annauniv.edu

¹ Refrigeration and Air-Conditioning Division, Department of Mechanical Engineering, Anna University, Chennai, Tamil Nadu 600 025, India

² International Institute for Carbon-Neutral Energy Research Kyushu University (WPI-I2CNER), 744 Motoooka, Nishi-ku, Fukuoka 819-0395, Japan

cooling system. Hence, there is a need for new and innovative heat transfer fluids to achieve high-performance cooling.

Over the past few decades, different nanomaterials are seeded with conventional heat transfer fluids in order to increase the thermal conductivity and energy transfer rate of such fluids. The nanomaterials are available with different shapes such as spherical, cylindrical and platelets. The spherical-shaped metallic and metallic oxide nanomaterials were used for the preparation of nanofluids with different basefluids, and enhancement of thermal conductivity has been summarized in the literature [1–4]. There is no promising enhancement in thermal conductivity with spherical nanoinclusions due to the high interfacial thermal resistance between the nanoparticles and the surrounding fluids [5, 6].

To avoid this issue, recently carbon-based cylindrical and platelet-shaped nanostructures are used to prepare high-conductivity nanofluids [7–11]. Experimental study on thermal conductivity with carbon-based nanostructures such as carbon nanotubes (CNTs) and graphene nanoplatelets (GnP) have been performed by several researchers [12–23]. Sabiha et al. [17] performed the thermal conductivity of SWCNT-H₂O nanofluids experimentally, and highest enhancement of thermal conductivity is reported to be ~36% for 0.25 vol%. The graphene nanoplatelets (GnP) could play a significant role in the enhancement of thermal conductivity due to its high thermal conductivity in the order of 3000–5000 W m⁻¹ K⁻¹. Amiri et al. [20] studied the thermal conductivity of GnP/H₂O–EG (H₂O:EG = 40:60) nanofluids experimentally and reported a 65% enhancement at ~0.1 vol%. From the above literature, it is possible to conclude that 2D nanoplatelets play a significant role in the enhancement of thermal conductivity compared to other dimensionalities. The GnPs (2D nanostructure) are highly beneficial due to their high thermal conductivity and high aspect ratio as compared to the 1D and spherical nanomaterials [24, 25]. Recent effective medium theory predictions and experimental results show that the GnP-based nanocomposites show a better thermal conductivity enhancement due to their low thermal boundary resistance as compared to the carbon nanotubes [26]. Enhancements in heat transfer coefficient using different nanofluids with spherical nanoparticles have been performed experimentally by several researchers [27–33]. The higher enhancement in heat transfer coefficient was found at higher volume concentration of the spherical nanoparticles in basefluid. This will increase viscosity of nanofluids significantly resulting in higher pressure drop. Many researchers have reported the enhancement of heat transfer coefficient by more than 50–100% at lower concentration (<1% itself) of 2D nanostructure with limited penalty in the pressure drop [23, 34–38]. It is clearly seen

that use of 2D nanostructure (GnP) with low density and high aspect ratio in basefluid will increase the thermal conductivity and heat transfer coefficient significantly.

The experimental studies on graphene nanoplatelets with water–ethylene glycol mixture are limited in the published literature. In order to understand the variation in thermophysical properties and thermal boundary resistance between graphene nanoplatelets and surrounding basefluids, further experimental works are required. In the current study, we report (1) thermophysical properties such as thermal conductivity and specific heat capacity of GnP/H₂O–EG nanofluids, (2) the enhancement in thermal conductivity of nanofluids and comparison of experimental data with predicted values based on effective medium theory predictions and (3) the interfacial thermal resistance between GnP and water–ethylene glycol mixture.

Materials and methods

In this work, graphene nanoplatelets (GnP) and water–ethylene glycol mixture (H₂O–EG) have been used as nanomaterial and basefluid, respectively. Generally, the water–ethylene glycol mixture with 30% volume of ethylene glycol is recommended to be used as a radiator coolant in winter [39]. Viscosity of water–ethylene glycol mixture will be increased when more quantity of ethylene glycol is added to the water. Hence, in the present study, we use water–ethylene glycol mixture (H₂O:EG = 70:30) as a base fluid which has lower freezing point and higher boiling point than pure water with minimum enhancement in viscosity value. Multilayered graphene nanoplatelets (GnP) were obtained from the XG Sciences, USA (Grade M, diameter: 15 μm, average thickness: 5–10 nm and density: 2.2 g cm⁻³). In the material used, the number of graphene layers varies from 10 to 30. Scanning electron microscope visualization (SEM) and transmission electron microscope visualization (TEM model JEOL, JEM-2000EX. Acceleration voltage 200 kV) of GnP are shown in Fig. 1a, b. The thermophysical properties and purity of materials and basefluids are listed in Table 1.

Due to the hydrophobic nature of GnP, we used of non-covalent functionalization to prepare stable dispersions. Covalent or non-covalent treatment is widely used to prepare stable nanofluid dispersions with carbon nanostructures. Covalent treatment using acids often damages the nanostructure and introduces structural defects in the planar structure of GnP. The intrinsic thermal conductivity of GnP will be reduced due to enhanced phonon scattering. To avoid this problem, non-covalent preparation method was used in this work.

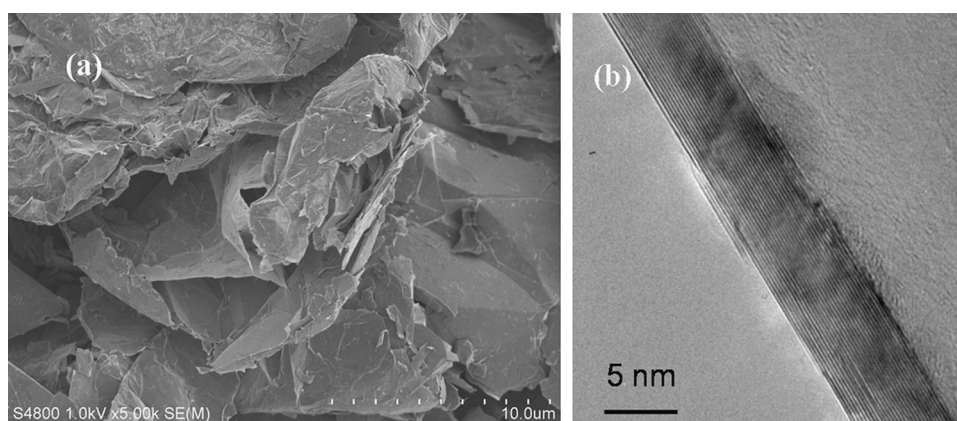


Fig. 1 **a** SEM and **b** TEM visualization of GnP

Table 1 Thermophysical properties and purity of materials and basefluids at 30 °C

Materials/Basefluids	Commercial source/prepared	Density/g cm ⁻³	Thermal conductivity/ W m ⁻¹ K ⁻¹	Mass fraction purity/%
Graphene nanoplatelets (Grade M)	XG sciences, USA	2.2 ^a	3000 ^a	99
Sodium Deoxycholate	Sigma Aldrich, USA	1.129 ^b	–	97
Ethylene glycol	Merck, USA	1.11 ^c	0.254 ± 0.0024 ^d	99
Deionized water	Lab chemicals, India	0.995 [40]	0.607 ± 0.015 ^d	99
H ₂ O–EG (70:30)	prepared	1.031 ± 0.01 ^d	0.456 ± 0.0045 ^d	99
H ₂ O–EG (70:30) + (0.75 vol % SDC)	prepared	1.045 ± 0.01 ^d	0.465 ± 0.0046 ^d	–

^a http://xgsciences.com/wp-content/uploads/2012/10/10-15-13_xGnP-M_Data-Sheet.pdf

^b <http://www.lookchem.com/Sodium-deoxycholate/>

^c http://www.merckmillipore.com/IN/en/product/Ethylene-glycol,MDA_CHEM-100949

^d Measured data with uncertainties for thermal conductivity and density are given in the table as expanded uncertainties with 0.95 level of confidence

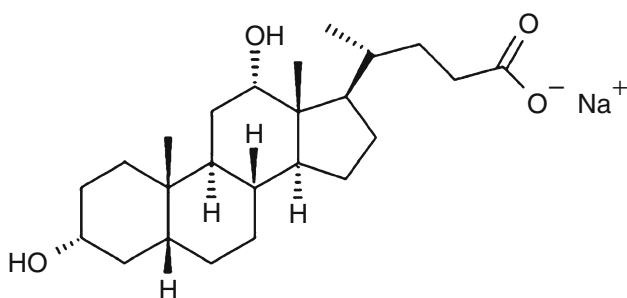


Fig. 2 Chemical structure of SDC (C₂₄H₃₉NaO₄)

In this work, sodium deoxycholate (SDC) surfactant (C₂₄H₃₉NaO₄, molecular weight: 414.55 g mol⁻¹) was used to prepare stable nanofluid dispersions. The molecular structure of SDC is shown in Fig. 2. Harish et al. [41] prepared SWCNT–H₂O nanofluids with SDC surfactant. Based on optical absorption spectroscopy and photoluminescence

spectroscopy studies, they reported that SDC is an effective surfactant to disperse hydrophobic nature materials in basefluids. Pure ethylene glycol was added to pure water in the volume (%) ratio 30:70 and stirred well for 30 min using magnetic stirrer. Sodium deoxycholate (SDC) surfactant with 0.75 vol% (0.82% by mass) was added to the water–ethylene glycol (H₂O–EG) mixture and stirred in the same way for 30 min. In this study, the basefluid (H₂O–EG) with 0.75 vol% SDC considered as 0 vol% nanofluid. The GnPs were added directly to the basefluid (H₂O–EG + 0.75 vol% SDC) by intensive ultrasonic vibration (QSonica, USA) for 2 h. The nanofluids were prepared with 0.001, 0.01, 0.05, 0.1, 0.15, 0.3 and 0.45% volume fractions of GnP (mass %: 0.0021, 0.021, 0.21, 0.42, 0.63, 0.83 and 1.04%). There was no visual sedimentation observed for the nanofluid suspensions kept undisturbed for more than 15 days. Furthermore, we also performed optical absorption (PG instruments, UK) and zeta potential (Horiba Nanopartica SZ-100, USA) measurements to investigate the stability of nanofluid dispersions.

Measurement of thermophysical properties

In this work, the thermal conductivity of nanofluids was measured using KD2 Pro thermal properties analyzer which works based on the transient hot wire method (Decagon Devices, USA). The KD2 Pro thermal properties analyzer is designed as per IEEE Standard 442–1981 and ASTM Standard D5334-08. In this instrument, the thermal conductivity of fluids can be measured with ks^{-1} sensor which is having an uncertainty of $\pm 5.0\%$ (for thermal conductivity ranges from 0.2 to 2 $W m^{-1} K^{-1}$). The thermal conductivity of nanofluid was measured at a temperature of 30 °C (± 0.15 °C accuracy) and normal atmosphere ($\pm 1\%$ accuracy).

Specific heat capacity of nanofluid was measured by differential scanning calorimeter (TA instruments, USA). The measurements were taken for the temperature ranging from 30 to 50 °C with a scanning rate of 0.015 °C min^{-1} . The combined uncertainty of specific heat measurements lies within $\pm 3\%$ deviation.

Results and discussion

Characterization of nanofluids

The prepared nanofluids were characterized by UV–Vis absorption spectrometer to predict the stability of dispersion. The stability test was performed for 15 days from the day of sample preparation for 0.01 vol% and 0.1 vol% of GnP loadings. Figure 3a illustrates the absorption spectra of GnP/H₂O–EG nanofluids for lower volume fraction GnP loadings which are performed on same day after the sample preparation. The absorbance is found to increase with respect to volume fraction of GnP. The maximum peak of the absorbance spectrum is found to be around 255 nm. Long-term stability test was carried out quantitatively using UV–Vis absorption spectrometer. The predicted relative concentrations of GnP/H₂O–EG nanofluids with respect to time are shown in Fig. 3b. The predicted relative concentration by absorbance at a wavelength of 255 nm is taken for time of 15 days with an interval of 5 days. It is found that the relative concentration of GnP/H₂O–EG nanofluids marginally decreases over a period of 15 days.

The reversibility characterization of prepared nanofluids was performed using UV–Vis absorption spectrometer. The prepared nanofluids are sonicated again for 30 min after 20 days in order to predict the reversible/irreversible characterization of dispersions. The comparison of UV–Vis spectrum of GnP/H₂O–EG nanofluids before sonication and after sonication is illustrated in Fig. 3c. The maximum sedimentation is found to be within 2% after sonication which indicates that the particle aggregation is reversible. From the UV–Vis results, it is observed that the prepared

nanofluids are stable for the experimentation. However, the particle agglomeration will be reversible during the circulation process in the heat transfer applications.

Zeta potential distribution

In order to confirm the stability of prepared nanofluid at higher volume fraction of GnP loadings, the zeta potential distribution analysis was carried out. Zeta potential measurement is taken on the 20th day of sample preparation with 30 min sonication and without sonication. Figure 4 illustrates the zeta potential distribution of the nanofluids before sonication at 0.45 vol% GnP as a function of intensity. The measured value of the electric potential at the slip plane between the bound layer of dilute molecules surrounding the particle and the bulk solution is known as zeta potential. Zeta potential distribution values are expected to be more positive than +30 mV or more negative than –30 mV in order to confirm the stability of solid–liquid dispersion [42]. The average zeta potential distribution value of nanofluid (0.45 vol% GnP) is found to be –43.8 mV. It is observed that the particles are highly electronegative which indicates a good stability of the prepared nanofluid dispersion. The average zeta potential distribution of the nanofluid with 0.45 vol% of GnP sonicated for 30 min was found to be –53.2 mV. It is clearly seen that the particle aggregation is reversible, and zeta potential distribution is more negative than –43.8 mV.

Calibration of measurement techniques

Initially, the measurements of thermal conductivity and specific heat capacity of water–ethylene glycol mixture (H₂O:EG = 70:30) were taken for the temperatures ranging from 30 to 50 °C. In order to calibrate the measurement techniques, the measured values were compared with the reference (ASHRAE standard) [43] values as listed in Table 2. It is found that the measured thermal conductivity and specific heat capacity values are in good agreement with the reference values within $\pm 2.5\%$.

Thermal conductivity

The measurement of thermal conductivity was taken at 30 °C on the same day after the sample preparation. At least 10 measurements were taken, and the average value was reported as the resultant thermal conductivity. Figure 5 illustrates the variation in thermal conductivity of nanofluids as a function of GnP loadings (vol%) at 30 °C. The thermal conductivity of nanofluids is found to increase significantly with respect to GnP loadings. Thermal conductivity is slightly enhanced (2%) even when the surfactant (SDC) added to the pure basefluid. Leong et al. [44] reported that

Fig. 3 **a** UV–Vis spectrum of GnP/H₂O–EG nanofluids, **b** the stability of GnP/H₂O–EG nanofluids with respect to time, **c** the reversibility characterization of GnP/H₂O–EG nanofluids with respect to time

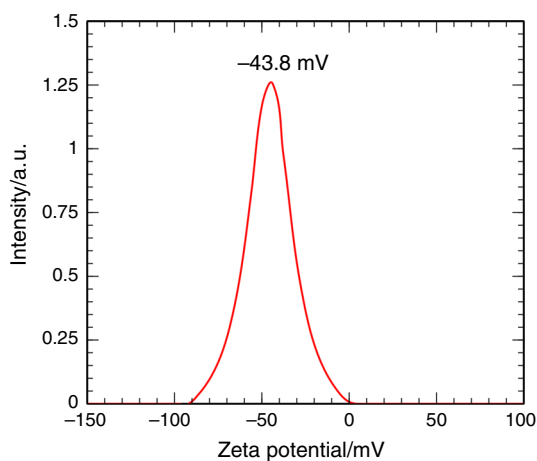
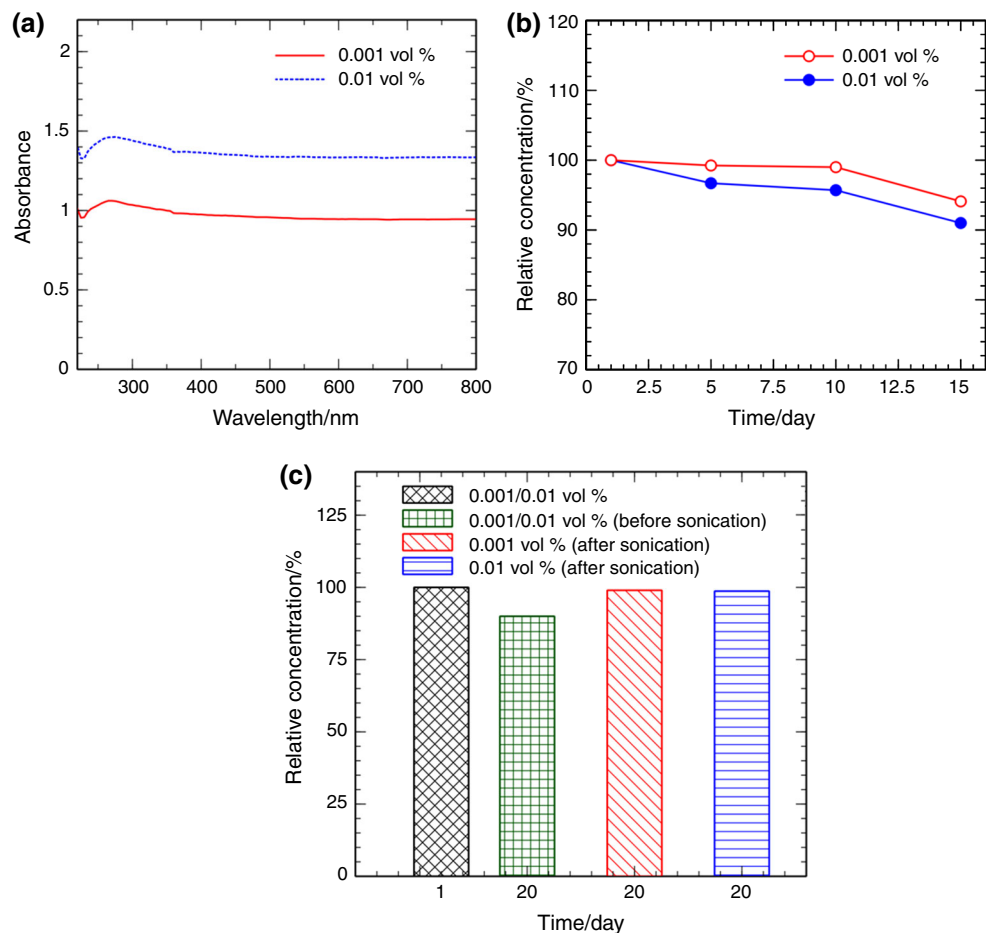


Fig. 4 Zeta potential distribution of (0.45 vol % GnP) nanofluids

the thermal conductivity of basefluid is enhanced up to 6.6% when gum Arabic surfactant was added to the basefluid. The highest enhancement of thermal conductivity is found to be $\sim 18\%$ at 0.45 vol%. Mechanism behind the thermal conductivity enhancement of nanofluids is still under debate. However, recent experimental works on freezing of nanofluid suspensions [45, 46] reveal that clustering of

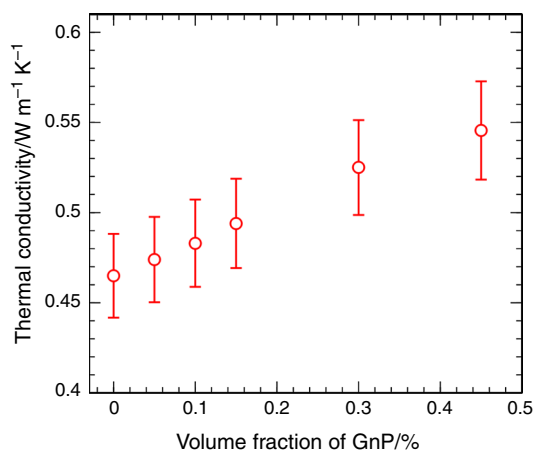
nanoparticles play a significant role in enhancing the thermal conductivity of suspensions. The works of Zheng et al. [45] and Harish et al. [46] show that the enhancement in thermal conductivity is significantly higher when clustering of nanoparticle is carefully controlled to form chain-like structures which enable efficient thermal transport thereby enhancing the thermal conductivity. Hence, it is possible that GnP with its 2D structure can form long chains which could be the reason for the significant enhancement in thermal conductivity even at very low loadings. Thermal conductivity measurement of nanofluid at higher concentration (0.45%) was taken after 20 days without sonication in order to check the repeatability. The thermal conductivity of 0.45 vol% GnP nanofluid is found to be $0.543 \pm 0.0055 \text{ W m}^{-1} \text{ K}^{-1}$. The result shows the 2.5% deviation as compared to the previous measurement due to error in the instrument. However, the deviation is negligible with respect to uncertainty in the measurement.

Furthermore, the measured thermal conductivity ratio (k_{nf}/k_{bf}) of GnP/H₂O–EG nanofluid is compared with those obtained from Maxwell–Garnett-type effective medium theory (EMT) model. Many parameters such as the nanoparticle shape, size, aspect ratio, volume concentration

Table 2 Comparison of measured data with reference data

Temperature/ °C	Thermal conductivity/W m ⁻¹ K ⁻¹		Specific heat capacity/kJ kg ⁻¹ K ⁻¹	
	Measured	Ref. [43]	Measured	Ref. [43]
30	0.456 ± 0.0045	0.455	3.604 ± 0.09	3.674
40	0.465 ± 0.0046	0.463	3.626 ± 0.09	3.702
50	0.473 ± 0.0047	0.471	3.673 ± 0.092	3.73

Measured data with uncertainties for thermal conductivity and specific heat capacity are given in the table as expanded uncertainties with 0.95 level of confidence

**Fig. 5** Thermal conductivity of GnP/H₂O-EG as a function of GnP loadings at 30 °C

and the interfacial thermal resistance between the nanomaterial and basefluid directly influence the enhancement in thermal conductivity. Nan et al. [47] proposed EMT model considering these parameters to predict the thermal conductivity enhancement. The thermal conductivity ratio (k_{nf}/k_{bf}) of nanofluid was determined using the following Eqs. (1–6).

$$\frac{k_{nf}}{k_{bf}} = \frac{3 + \phi[2\beta_{11}(1 - L_{11}) + \beta_{33}(1 - L_{33})]}{3 - \phi[2\beta_{11}L_{11} + \beta_{33}L_{33}]} \quad (1)$$

where the dimensionless parameters β_{11} , β_{33} , L_{11} and L_{33} are defined as follows in Eqs. (2–4)

$$\beta_{11} = \frac{k_{11}^c - k_{bf}}{k_{bf} + L_{11}(k_{11}^c - k_{bf})}, \beta_{33} = \frac{k_{33}^c - k_{bf}}{k_{bf} + L_{33}(k_{33}^c - k_{bf})} \quad (2)$$

$$L_{11} = \frac{a^2}{2(a^2 - 1)} - \frac{a^2}{2(1 - a^2)^{3/2}} \text{Cos } h^{-1} a \quad (3)$$

$$L_{33} = 1 - 2L_{11} \quad (4)$$

where k_{nf} and k_{bf} refer to thermal conductivity of nanofluid and basefluid, respectively. ϕ is the volume fraction of graphene nanoplatelets inclusions. L_{11} and L_{33} are geometric shape factors of the spheroid particle. a ($a = l/t$) is the aspect ratio of ellipsoid (l and t are length and thickness

of graphene nanoplatelets inclusions, respectively). k_{11}^c and k_{33}^c are refer to the equivalent thermal conductivity of the composite along the longitudinal and transverse directions.

The equivalent thermal conductivities of the composite considering the role of thermal interface resistance can be estimated as follows:

$$k_{ii}^c = \frac{k_p}{1 + \frac{\gamma L_{ii} k_p}{k_{bf}}}, \quad i = 1, 3 \quad (5)$$

With

$$\gamma = (1 + 2a) \frac{R k_{bf}}{t} \quad (6)$$

where k_p and R refer to the thermal conductivity of GnP and the interfacial thermal resistance between the GnP and basefluid, respectively.

For model calculations, the length and thickness of GnP are considered to be 1 μm and 10 nm, respectively. The thermal conductivity of the GnP is considered to be 3000 W m⁻¹ K⁻¹. The interfacial thermal resistance between GnP and basefluid is determined using the EMT model.

Figure 6 illustrates the comparison of measured thermal conductivity enhancement with those obtained from the EMT model predictions. The interfacial thermal resistance is extracted from the EMT model for the present experimental conditions and parameters. The measured thermal conductivity data are in good agreement with the EMT model predictions. The interfacial thermal resistance between graphene nanoplatelets and water–ethylene glycol mixture is found to be $1.7 \times 10^{-8} \text{ m}^2 \text{KW}^{-1}$. The thermal conductivity enhancement is significantly increased, when the interfacial thermal resistance is considered as 0 $\text{m}^2 \text{KW}^{-1}$ is shown in Fig. 6. Hence, it is found that the interfacial thermal resistance is limiting the enhancement of thermal conductivity. The thermal boundary conductance (inverse of interfacial thermal resistance) of GnP/H₂O-EG nanofluid is found to be $\sim 60 \text{ MW m}^2 \text{K}^{-1}$ from EMT prediction. Konatham et al. [48] studied the thermal conductivity enhancement of graphene–organic interfaces nanofluids. The maximum thermal boundary conductance of nanofluids is reported to be in the range of

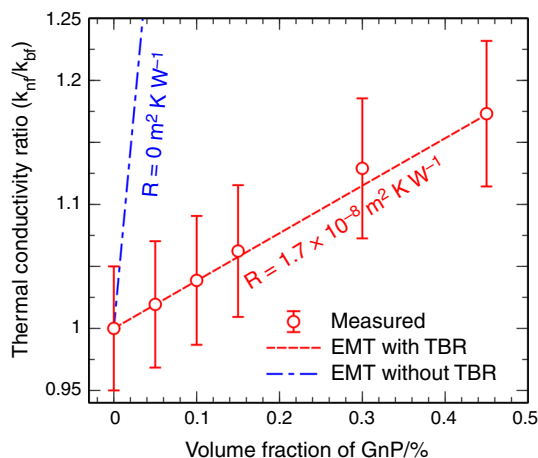


Fig. 6 Comparison of thermal conductivity enhancement with EMT model predictions

50–270 MW m² K⁻¹. The thermal boundary conductance (TBC) of present nanofluid is in good agreement within the range reported in the published literature [48]. The GnP/H₂O–EG nanofluids show better thermal performance than the carbon nanotube-based nanofluids due to its high TBC. Carbon nanotube-based nanofluids have a very low TBC in the range of 2.4–12 MW m² K⁻¹ [49] which indicates the graphene nanoplatelets are highly beneficial as compared to CNTs.

Specific heat capacity

Figure 7 illustrates the variation of specific heat capacity with respect to volume fraction of GnP loadings at 30 °C. The specific heat of nanofluid is found to decrease with increase in GnP loadings. The specific heat capacity of the nanofluid reduces with addition of GnP due to lower specific heat capacity of GnP as compared to the basefluid. The highest decrement in specific heat is found to be ~8% for 0.45 vol% as compared to 0 vol%. Further, the measured specific heat capacity of GnP nanofluid is compared with those obtained from physical principle of mixture rule as given in Eq. (7).

$$(C_p)_{nf} = \frac{(1 - \phi_P)(\rho C_p)_{bf} + \phi_P(\rho C_p)_P}{(1 - \phi_P)\rho_{bf} + \phi_P\rho_P} \quad (7)$$

For model calculation, the specific heat capacity of GnP and basefluid (0 vol%) is considered to be 0.643 [50] and 3.43 kJ kg⁻¹ K⁻¹, respectively.

The comparison of measured specific heat capacity with mixture rule is illustrated in Fig. 7. It is clearly seen that the measured specific heat capacity of nanofluids are lower than those of the predicted values using mixture rule. It is observed that the specific heat capacity marginally reduces with respect to GnP loadings which is obtained from mixture rule. The variation of specific heat capacity lies

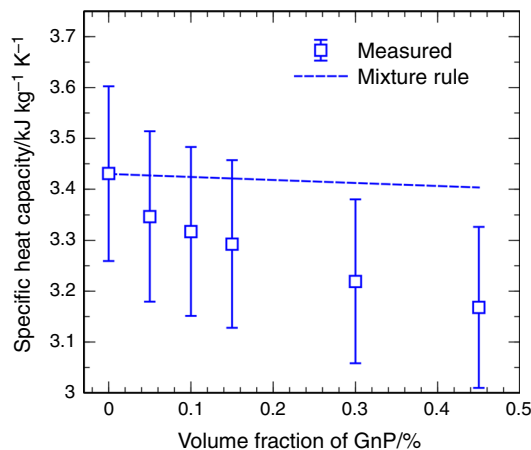


Fig. 7 Specific heat capacity of GnP/H₂O–EG as a function of GnP loadings at 30 °C

within the error limits up to 0.15 vol% of GnP loadings, while beyond 0.15 vol% of GnP the deviation exceeds the error bandwidth. Rule of mixtures was developed based on thermal equilibrium between the nanoparticles and basefluid. The dispersion of nanoparticles in basefluid leads to the faster propagation of heat into and out of the medium due to the enhancement in thermal diffusivity. It is inferred that nanoparticles and basefluid are not in thermal equilibrium due to enhancement in thermal diffusivity [51]. Hence, the deviation is higher between the measured values and predicted values using mixture rule.

Conclusions

The GnP/H₂O–EG nanofluids were prepared by non-covalent method, and their thermal properties such as thermal conductivity and specific heat capacity were measured experimentally. The UV–Vis absorption spectrum and zeta potential analyses were performed in order to confirm the stability of the prepared nanofluid dispersions. From the results, it is found that the prepared nanofluid was stable. Thermal conductivity of nanofluid significantly increases with increasing volume concentration of graphene nanoplatelets loading. The highest enhancement of thermal conductivity was found to be ~18% at 0.45 vol% of GnP, respectively. The measured thermal conductivities of GnP/H₂O–EG nanofluids were compared with those predicted using Maxwell–Garnett-type effective medium theory. The interfacial thermal resistance between graphene nanoplatelets and water–ethylene glycol mixture was estimated to be 1.7×10^{-8} m² K W⁻¹. A study on reducing the interfacial thermal resistance between graphene nanoplatelets and base fluid to further enhance the thermal conductivity of nanofluid could be a topic for further research.

Acknowledgements Selvam and Mohan lal acknowledge the University Grants Commission (UGC), India, for the financial support (F.NO. 42-896/2013 (SR), Date- 25.3.13) toward conducting this study. Harish acknowledges the support of JSPS kakenhi 16H07043.

References

- Fan J, Wang L. Review of heat conduction in nanofluids. *J Heat Transf.* 2011;133:040801–13.
- Angayarkanni SA, Philip J. Review on thermal properties of nanofluids: recent developments. *Adv Colloid Interface Sci.* 2015;225:146–76.
- Azmi WH, Sharma KV, Mamat R, Najafi G, Mohamad MS. The enhancement of effective thermal conductivity and effective dynamic viscosity of nanofluids—a review. *Renew Sust Energy Rev.* 2016;53:1046–58.
- Devendiran DK, Amirtham VA. A review on preparation, characterization, properties and applications of nanofluids. *Renew Sust Energy Rev.* 2016;60:21–40.
- Buongiorno J, et al. A benchmark study on the thermal conductivity of nanofluids. *J Appl Phys.* 2009;106:1–14.
- Huxtable ST, Cahill DG, Shenogin S, Xue L, Ozisik R, Barone P, Usrey M, Strano MS, Siddons G, Shim M, Keblinski P. Interfacial heat flow in carbon nanotube suspensions. *Nat Mater.* 2003;2:731–4.
- Xie H, Chen L. Review on the preparation and thermal performances of carbon nanotube contained nanofluids. *J Chem Eng Data.* 2011;56:1030–41.
- Sohel Murshed SM, Nieto de Castro CA. Superior thermal features of carbon nanotubes-based nanofluids—A review. *Renew Sust Energy Rev.* 2014;37:155–67.
- Sadeghinezhad E, Mehrali M, Saidur R, Mehrali M, Tahan Latibari S, Reza Akhiani A, Cornelis Metselaar HS. A comprehensive review on graphene nanofluids: recent research, development and applications. *Energy Convers Manag.* 2016;111:466–87.
- Rasheed AK, Khalid M, Rashmi W, Gupta TCSM, Chan A. Graphene based nanofluids and nanolubricants—Review of recent developments. *Renew Sust Energy Rev.* 2016;63:346–62.
- Gogotsi Y. Graphene in composite materials: synthesis, characterization and applications. *Carbon.* 2013;61:650–1.
- Choi SUS, Zhang ZG, Yu W, Lockwood FE, Grulke EA. Anomalous thermal conductivity enhancement in nanotube suspensions. *Appl Phys Lett.* 2001;79:2252–4.
- Ding Y, Alias H, Wen D, Williams RA. Heat transfer of aqueous suspensions of carbon nanotubes (CNT nanofluids). *Int J Heat Mass Transf.* 2006;49:240–50.
- Harish S, Ishikawa K, Einarsson E, Aikawa S, Shiomi SCJ, Maruyama S. Enhanced thermal conductivity of ethylene glycol with single-walled carbon nanotube inclusions. *Int J Heat Mass Transf.* 2012;55:3885–90.
- Ghozatloo A, Rashidi AM, Niasar MS. Effects of surface modification on the dispersion and thermal conductivity of CNT/water nanofluids. *Int Commun Heat Mass Transf.* 2014;54:1–7.
- Shanbedi M, Heris SZ, Maskooki A. Experimental investigation of stability and thermophysical properties of carbon nanotubes suspension in the presence of different surfactants. *J Therm Anal Calorim.* 2015;120:1193–201.
- Sabiha MA, Mostafizur RM, Saidur R, Mekhilef S. Experimental investigation on thermo physical properties of single walled carbon nanotube nanofluids. *Int J Heat Mass Transf.* 2016;93:862–71.
- Jyothirmayee Aravind SS, Ramaprabhu S. Surfactant free graphene nanoplatelets based nanofluids by in situ reduction of alkaline graphite oxide suspensions. *J Appl Phys.* 2011;110:12326-1–5.
- Yu W, Xie H, Wang X, Wang X. Significant thermal conductivity enhancement for nanofluids containing graphene nanoplatelets. *Phys Lett A.* 2011;375:1323–8.
- Amiri A, Sadri R, Shanbedi M, Ahmadi G, Kazi SN, Chew BT, Mohd Zubir MN. Synthesis of ethylene glycol-treated graphene nanoplatelets with one-pot, microwave-assisted functionalization for use as a high performance engine coolant. *Energy Convers Manag.* 2015;101:767–77.
- Sarsam WS, Amiri A, Kazi SN, Badarudin A. Stability and thermophysical properties of non-covalently functionalized graphene nanoplatelets nanofluids. *Energy Convers Manag.* 2016;116:101–11.
- Ahamed N, Asirvatham LG, Titus J, Bose JR, Wongwises S. Measurement of thermal conductivity of graphene–water nanofluid at below and above ambient temperatures. *Int Commun Heat Mass Transf.* 2016;70:66–74.
- Arzani HK, Amiri A, Arzani HK, Rozali SB, Kazi SN, Badarudin A. Toward improved heat transfer performance of annular heat exchangers with water/ethylene glycol based nanofluids containing graphene nanoplatelets. *J Therm Anal Calorim.* 2016;. doi:10.1007/s10973-016-5663-8.
- Marconnet AM, Panzer MA, Goodson KE. Thermal conduction phenomena in carbon nanotubes and related nanostructured materials. *Rev Mod Phys.* 2013;85:1295–326.
- Balandin AA. Thermal properties of graphene and nanostructured carbon materials. *Nat Mater.* 2011;10:569–81.
- Harish S, Orejon D, Takata Y, Kohno M. Thermal conductivity enhancement of lauric acid phase change nanofluid with graphene nanoplatelets. *Appl Therm Eng.* 2015;80:205–11.
- Wen D, Ding Y. Experimental investigation into convective heat transfer of nanofluids at the entrance region under laminar flow conditions. *Int J Heat Mass Transf.* 2004;47:5181–8.
- Kulkarni DP, Namburu PK, Ed Bargar H, Das DK. Convective heat transfer and fluid dynamic characteristics of SiO₂ ethylene glycol/water nanofluid. *Heat Transf Eng.* 2008;29:1027–35.
- Kim D, Kwon Y, Cho Y, Li C, Cheong S, Hwang Y, Lee J, Hong D, Moon S. Convective heat transfer characteristics of nanofluids under laminar and turbulent flow conditions. *Curr Appl Phys.* 2009;9:e119–23.
- Peyghambarzadeh SM, Hashemabadi SH, Hoseini SM, Seifi Jamnani M. Experimental study of heat transfer enhancement using water/ethylene glycol based nanofluids as a new coolant for car radiators. *Int Commun Heat Mass Transf.* 2011;38:1283–90.
- Heyhat MM, Kowsary F, Rashidi AM, Alem Varzane Esfehiani S, Amrollahi A. Experimental investigation of turbulent flow and convective heat transfer characteristics of alumina water nanofluids in fully developed flow regime. *Int Commun Heat Mass Transf.* 2012;39:1272–8.
- Yu W, Xie H, Li Y, Chen L, Wang Q. Experimental investigation on the heat transfer properties of Al₂O₃ nanofluids using the mixture of ethylene glycol and water as base fluid. *Powder Technol.* 2012;230:14–9.
- Madhesh D, Kalaiselvam S. Experimental study on the heat transfer and flow properties of Ag–ethylene glycol nanofluid as a coolant. *Heat Mass Transf.* 2014;50:1597–607.
- Sadeghinezhad E, Mehrali M, Latibari ST, Mehrali M, Kazi SN, Sean Oon C, Metselaar HSC. Experimental investigation of convective heat transfer using graphene nanoplatelet based nanofluids under turbulent flow conditions. *Ind Eng Chem Res.* 2014;53:12455–65.
- Arzani HK, Amiri A, Kazi SN, Chew BT, Badarudin A. Experimental and numerical investigation of thermophysical properties, heat transfer and pressure drop of covalent and non-covalent functionalized graphene nanoplatelet-based water nanofluids in an annular heat exchanger. *Int Commun Heat Mass Transf.* 2015;68:267–75.

36. Mehrali M, Sadeghinezhad E, Rosen MA, Latibari ST, Mehrali M, Metselaar HSC, Kazi SN. Effect of specific surface area on convective heat transfer of graphene nanoplatelet aqueous nanofluids. *Exp Thermal Fluid Sci.* 2015;68:100–8.
37. Amiri A, Sadri R, Shanbedi M, Ahmadi G, Kazi SN, Chew BT, Mohd Zubir MN. Synthesis of ethylene glycol-treated graphene nanoplatelets with one-pot, microwave-assisted functionalization for use as a high performance engine coolant. *Energy Convers Manag.* 2015;101:767–77.
38. Amiri A, Shanbedi M, Chew BT, Kazi SN, Solangi KH. Toward improved engine performance with crumpled nitrogen-doped graphene based water–ethylene glycol coolant. *Chem Eng J.* 2016;289:583–95.
39. Nunney MJ. *Automotive technology*. 3rd ed. Michigan: SAE International; 1998.
40. McLinden MO, Klein SA, Lemmon EW, Peskin AP. NIST thermodynamic and transport properties of refrigerant mixtures—REFPROP, Version 6.01, NIST Standard Reference Database 23, National Institute of Standards and Technology, Gaithersburg, MD, 1998.
41. Harish S, Ishikawa K, Einarsson E, Aikawa S, Inoue T, Zhao P, Watanabe M, Chiashi S, Shiomi J, Maruyama S. Temperature dependent thermal conductivity increase of aqueous nanofluid with single walled carbon nanotube inclusion. *Mater Express.* 2012;2:213–23.
42. Park S, Ruoff RS. Chemical methods for the production of graphenes. *Nat Nanotechnol.* 2009;4:217–24.
43. ASHRAE Handbook, Fundamentals, American Society of Heating, Refrigerating and Air-Conditioning Engineers Inc., Atlanta, GA, 2013.
44. Leong KY, Mohd Hanafi N, Mohd Sohaimi R, Amer NH. The effect of surfactant on stability and thermal conductivity of carbon nanotube based nanofluids. *Thermal Sci.* 2016;20:429–36.
45. Zheng R, Gao JW, Wang JJ, Chen G. Reversible temperature regulation of electrical and thermal conductivity using liquid-solid phase transitions. *Nat Commun.* 2011;2:1–6.
46. Harish S, Ishikawa K, Chiashi S, Shiomi J, Maruyama S. Anomalous thermal conduction characteristics of phase change composites with single-walled carbon nanotube inclusions. *J Phys Chem C.* 2013;117:15409–13.
47. Nan CW, Birringer R, Clarke DR, Gleiter H. Effective thermal conductivity of particulate composites with interfacial thermal resistance. *J Appl Phys.* 1997;81:6692–9.
48. Konatham D, Striolo A. Thermal boundary resistance at the graphene-oil interface. *Appl Phys Lett.* 2009;95:163105-1–3.
49. Kang Kim K, Hsu A, Jia X, Min Kim S, Shi Y, Dresselhaus M, Jing Kong TP. Synthesis and characterization of hexagonal boron nitride film as a dielectric layer for graphene devices. *ACS Nano.* 2012;6:8583–90.
50. Hone J. Phonons and thermal properties of carbon nanotubes. *Top Appl Phys.* 2001;80:273–86.
51. Vajjha RS, Das DK. Specific Heat Measurement of Three Nanofluids and Development of New Correlations. *J Heat Transf.* 2009;131:071601–7.